Temperature dependence of intra-stack defect spin–conduction-electron spin interaction in fluoranthene and perylene radical cation salts

Temperature dependence of intra-stack defect spin–conduction-electron spin interaction in fluoranthene and perylene radical cation salts

B Pongs and E Dormann

Physikalisches Institut, Universität Karlsruhe (TH), D-76128 Karlsruhe, Germany

E-mail: edo@piobelix.physik.uni-karlsruhe.de

Abstract
The electron spin resonance line-width anisotropy and intensity are analysed for the quasi-one-dimensional organic conductors $(fluoranthene)_2PF_6$ and $(perylene)_2PF_6 \cdot 2/3$ tetrahydrofurane in the metallic phase above the Peierls transition temperature. Based on the bottleneck model of relaxation, the temperature dependence of the intra-stack exchange constant between conduction-electron spins and localized defect spins is derived and discussed.

1. Introduction

Quasi-one-dimensional organic conductors like the fluoranthene radical cation salts $(FA)_2PF_6$ show an extremely narrow electron spin resonance (ESR) line-width in the metallic high-temperature phase [1]. For temperatures markedly higher than the Peierls transition temperature T_P, the ESR line-width and the respective longitudinal and transversal relaxation times, T_1 and T_2, exhibit just a minor orientation dependence [1–5]. Below the Peierls transition temperature T_P, i.e. in the charge density wave (CDW) ordered state, an increase in line-width and relaxation rates for decreasing temperature is generally observed for conducting radical cation salts built up from one-dimensional stacks of aromatic pure hydrocarbon molecules [3–6]. In this temperature range the magnetic dipolar interaction between localized paramagnetic defects and the conduction electrons of the same stack gives rise to the observed anisotropies. A bottleneck situation explains the peculiar orientation and temperature dependences. The defect spins do not relax directly to the lattice but via exchange interaction to the conduction electrons, which also have a weak spin–orbit coupling as well as slow spin lattice relaxation, thus causing back-relaxation and the bottleneck situation mentioned above. In the low-temperature phase of the arene radical cation salts, the temperature dependence of the conduction-electron magnetic susceptibility is rather pronounced due to the widening of the energy gap at $T < T_P$ and, with satisfactory accuracy, the observed line broadening and anisotropies could be described quantitatively based on the assumption that the intra-stack exchange integral between the defect

spin and conduction-electron spin is independent of temperature, i.e. $J_{DC}(T) = $ constant for $T < T_P$ [3, 4].

Recently, for a pyrene (PY) radical cation salt with an especially large anisotropy in its microwave electrical conductivity, i.e. $(PY)_{12}(SbF_6)_7$, we realized that the ESR line-width anisotropy can be described in the metallic high-temperature phase along the same lines as for the low-temperature phase. An exponential decrease in the exchange constant with increasing temperature, i.e. $J_{DC}(T) = J_0 \exp(-\text{constant} \times T)$, was deduced for $T > T_P$ [8]. This observation stimulated the ESR investigations reported below. For the fluoranthene radical cation salt $(FA)_2PF_6$ and the perylene salt $(PE)_2PF_6 \cdot 2/3THF$ (THF: tetrahydrofurane) we measured the ESR line susceptibility and the anisotropy of the width at $T > T_P$ and derived the temperature dependence of the respective intra-stack exchange constants.

2. Crystal growth and crystal structure

The crystals $(FA)_2PF_6$ and $(PE)_2PF_6 \cdot 2/3THF$ were grown by anodic oxidation, as described previously in [4, 7]. The principle organization of the crystal structure of these radical cation salts is similar: the flat arene molecules form stacks and the counter-ions are located in channels between these stacks. The overlap of the π orbitals of the carbon molecules of neighbouring arene molecules and the charge transfer from the arenes to the counter-ions give rise to a one-dimensional conduction band in the stacking direction. From measurements of the static magnetic susceptibility, we know that the crystals contain about 10^{-4} and 10^{-3} paramagnetic defects per formula unit for fluoranthene and perylene, respectively [2, 4]. The ESR signal in the metallic range thus arises from the conduction electrons, but it is strongly influenced by their magnetic interaction with the paramagnetic defects.

3. Experimental details and results

3.1. Angular dependence of the electron spin resonance line-width

All ESR measurements were performed at the X band (i.e. at about 9.45 GHz) using a Bruker ESP 300E spectrometer. Since there had been a prior detailed analysis of the line-shape and the absolute value of the line-width of the ESR absorption line for the fluoranthene salt as well as for the perylene salt [2, 4, 5], in this report we focus on the angular dependence of the ESR line-width (half width at half maximum (HWHM), $\Delta B_{1/2}$) in the temperature range above and around the Peierls transition temperature, T_P.

Figure 1 shows the values of $\Delta B_{1/2}$ for a $(FA)_2PF_6$ and a $(PE)_2PF_6 \cdot 2/3THF$ crystal as a function of the angle Θ between the static magnetic field and the crystal axis a at different temperatures. The a direction corresponds to the stacking direction of the arene molecules. As is known from the low-temperature analysis of the line-width, this angular dependence is caused by dipole–dipole-interaction between the conduction electrons and the localized paramagnetic defects in the arene stack, consequently the maximum of $\Delta B_{1/2}$ is observed for magnetic fields in the stacking direction.

The solid curves in figure 1 are fits using the formula

$$\Delta B_{1/2} = \Delta B_0 + d\left\{\tfrac{3}{8}(1 - 3\cos^2\Theta)^2 J(0) + \tfrac{15}{14}\sin^2\Theta\cos^2\Theta J(\omega) + \tfrac{3}{8}\sin^4\Theta J(2\omega)\right\} \qquad (1)$$

where $J(\omega) = 2\tau/(1 + \omega^2\tau^2)$ (which should be distinguished from the exchange constant $J_{DC}(T)$) is the spectral density, assuming an exponential decay in the correlation between the spins, with a correlation time τ. The validity of equation (1) was also checked through variation of the Larmor frequency ω at constant T [8]. The strength of the dipolar coupling is described
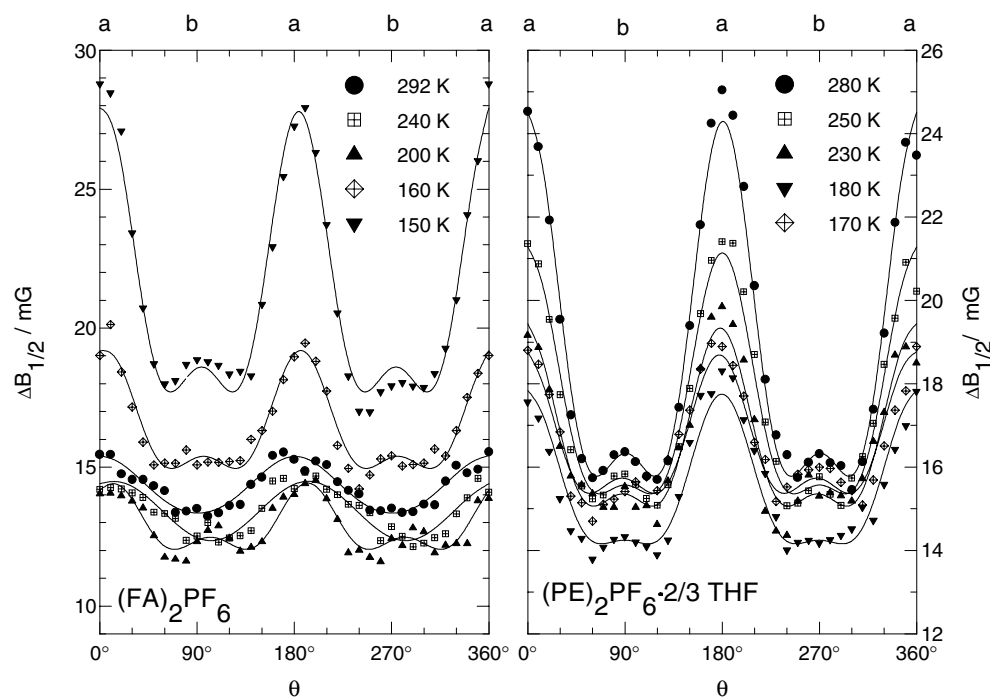
Figure 1. The angular dependency of the ESR line-width (HWHM) at various temperatures. The '*a* direction' with the line-width maximum corresponds to the stacking axis of the arene molecules, i.e. to the highly conducting direction.

by the parameter $d = (\gamma^3 \hbar^2 S(S+1))/r^6$, which depends primarily on the average distance between the interacting spins r. We have shown previously [8] that the value of r^6 changes by less than 10% over the investigated temperature range, so d can be considered to be nearly temperature independent. Table 1 shows typical values of the correlation time τ and d for the perylene and fluoranthene salts, as well as for the $(PY)_{12}(SbF_6)_7$ salt that was investigated previously [8]. For example, for the latter salt, the value d corresponds to an average separation of $(\langle r^{-6} \rangle)^{-1/6} = 28.6$ Å, i.e. about 8.5 times the typical intra-stack molecule separation. The parameter d can also be interpreted as $d = c(\gamma^3 \hbar^2 S(S+1))/r_{min}^6$, where c yields the probability that the conduction electron reaches the nearest-neighbour position r_{min} of the defect spin [3]. This probability amounts to only about 6×10^{-5} for the FA and PE salts (see table 1).

3.2. Bottleneck model

As mentioned above, the spin dynamics of the arene radical cation salts are governed by a bottleneck situation: the relaxation from defect spins and conduction-electron spins to the crystal lattice is much slower than the mutual relaxation between the two kinds of spins. The relaxation process between the paramagnetic defect spins and the conduction-electron spins therefore obeys a detailed balance condition:

$$\left(\frac{1}{T_1}\right)_{DC} \chi_D = \left(\frac{1}{T_1}\right)_{CD} \chi_C \qquad (2)$$
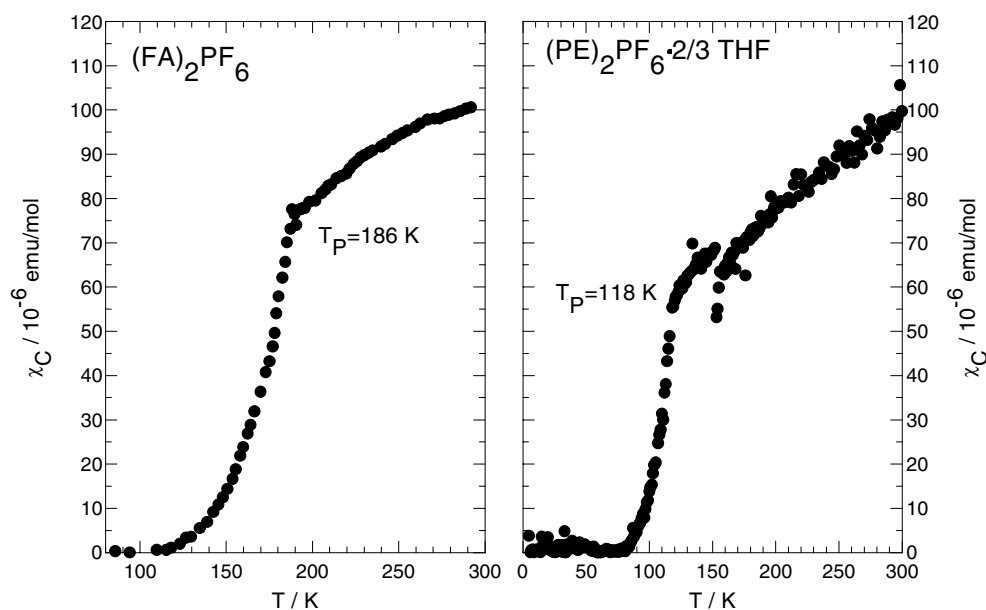
Figure 2. The temperature dependence of the conduction-electron susceptibility, χ_C, which was calculated from measurements of the total static magnetic susceptibility by subtracting the diamagnetic part and the part of the paramagnetic defects [3, 9].

Table 1. Results for the Peierls transition temperature T_P, the strength d and the correlation time τ of the dipole–dipole-interaction at $T = 250$ K, obtained by fitting equation (1) to the measured angular dependences of the ESR line-width.

	$(FA)_2PF_6$	$(PE)_2PF_6\cdot2/3THF$	$(PY)_{12}(SbF_6)_7$
T_P (K)	186	118	116
d (G s^{-1})	1.82×10^8	2.2×10^8	$8.3 \times 10^{6\,a}$
τ (250 K) (s)	5.6×10^{-11}	1.9×10^{-11}	$2.61 \times 10^{-10\,a}$
$J_{DC}(T < T_P)$ (meV)	121.0	220.0	16.25
Q (K^{-1})	0.030	0.011	0.013

[a] The values for the PY salt were measured at 420 MHz [8].

where χ_C is the magnetic susceptibility of the conduction electrons (figure 2) and χ_D is the magnetic susceptibility of the localized paramagnetic defects. Both were derived from superconducting quantum interference device (SQUID) magnetometer measurements of the total static magnetic susceptibility [3, 4] and verified by ESR intensity measurements. The relaxation rates $(1/T_1)_{DC}$ and $(1/T_1)_{CD}$ (i.e. the relaxation rates from the defect spins to the conduction electrons, and vice versa) make up the time limit for the correlation time of the dipole–dipole interaction, τ, of equation (1):

$$\frac{1}{\tau} = \left(\frac{1}{T_1}\right)_{DC} + \left(\frac{1}{T_1}\right)_{CD} \approx \left(\frac{1}{T_1}\right)_{DC}. \tag{3}$$

The latter approximation is valid, since our analysis is restricted to the temperature range around and above the Peierls transition temperature, where the conduction electron susceptibility (figure 2) is much larger than the susceptibility of the paramagnetic defects, which obey a Curie law.
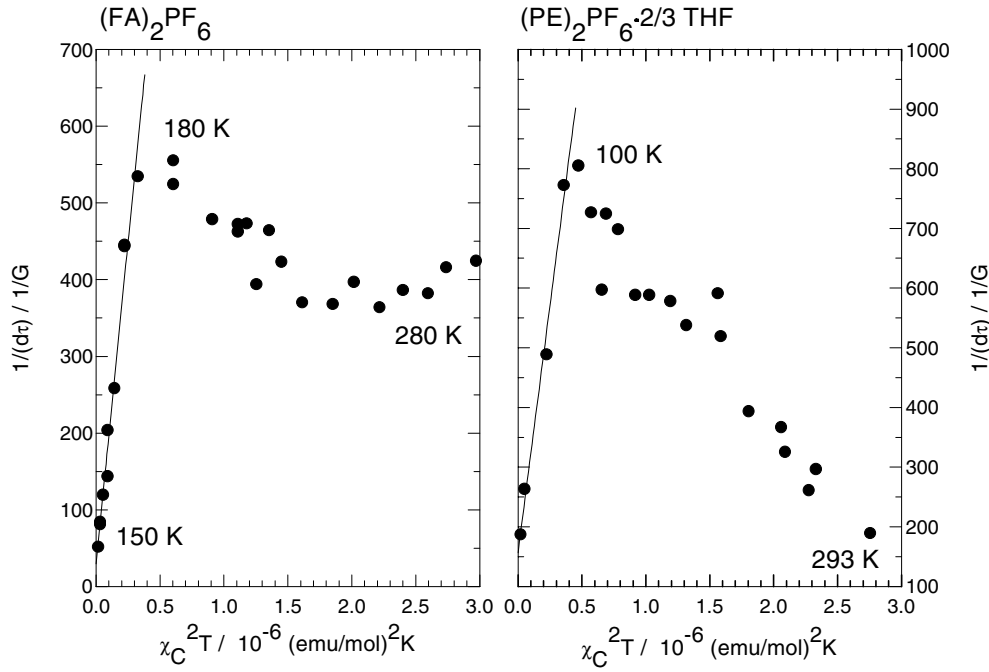
Figure 3. The dependence of $1/d\tau$ on $\chi_C^2 T$, with temperature T as an implicit parameter. For $T < T_P$ the measured data show linear behaviour, as one would expect from equation (5) with a temperature-independent exchange coupling constant, J_{DC}.

We have shown before that the predominant relaxation process for $(1/T_1)_{DC}$ is the exchange coupling between the localized defect spins and the conduction electrons [4, 8]. It can be described in analogy to the Korringa relaxation of nuclei in metals [10]:

$$\frac{1}{\tau} \approx \left(\frac{1}{T_1}\right)_{DC} = \frac{\pi k_B}{\hbar \mu_B^4} J_{DC}^2 \chi_C^2 T. \tag{4}$$

We finally obtain the following expression for the temperature dependence of the experimentally determined values of $d\tau$:

$$\frac{1}{d\tau} = \frac{\pi k_B r^6}{\hbar^3 \gamma^3 \mu_B^4 S(S+1)} J_{DC}^2 \chi_C^2 T + \left(\frac{1}{d\tau}\right)_0 \tag{5}$$

where $(1/d\tau)_0$ is an empirically introduced small constant term, which proved necessary for a correct description of $d\tau$ in the low-temperature phase of arene salts (see figure 3 [4, 8]).

Figure 3 shows the experimental data of $1/d\tau$ for $(FA)_2PF_6$ and $(PE)_2PF_6 \cdot 2/3THF$ as a function of $\chi_C^2 T$. One can clearly see that the linear correlation one would expect for a temperature-independent exchange coupling constant, J_{DC}, is fulfilled for temperatures lower than the respective Peierls transition temperature, T_P (table 1). At higher temperatures, however, the measured data show completely different behaviour. Since there is no reason why the applied theory should not be valid in the high-temperature regime, we conclude that there must be a temperature dependence in the exchange coupling 'constant', J_{DC} (as mentioned above, the temperature dependence of the distance, r, between the interacting defect and conduction electron spins is negligible).
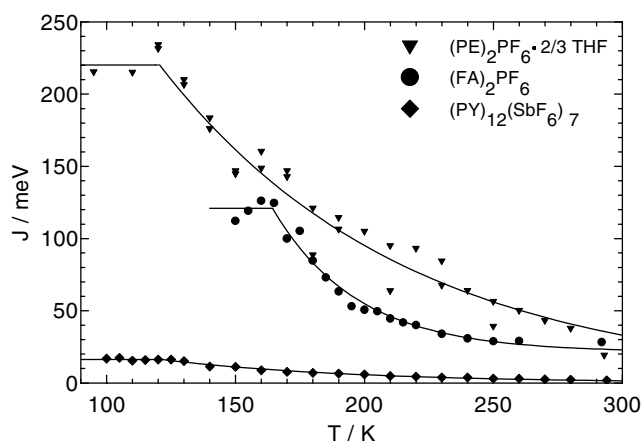
Figure 4. The temperature dependence of the exchange coupling constant J_{DC} (referring to one arene molecule) for the three samples that were investigated. The solid curves are explained in the text. For $(PY)_{12}(SbF_6)_7$, see [8].

3.3. Temperature dependence of the exchange constant

Using equation (5) and the measured conduction-electron susceptibility χ_C (figure 2), one can easily calculate the temperature dependence of the exchange coupling constant J_{DC} from the measured values of $d\tau$. The results for the $(FA)_2PF_6$ sample and the $(PE)_2PF_6 \cdot 2/3THF$ sample are shown in figure 4, together with the result for the $(PY)_{12}(SbF_6)_7$ salt [8]. The absolute value of J_{DC} refers to one arene molecule. At first, J_{DC} increases with decreasing temperature for all samples and becomes temperature independent (exaggerated as a break in slope in figure 4) in the temperature range around T_P, i.e. when the Peierls distortion of the crystal lattice locks in. As we have found already for the PY salt, the increase in J_{DC} shows exponential behaviour:

$$J_{DC}(T) = J_0 e^{-Q \cdot T} + J_1. \tag{6}$$

This temperature dependence corresponds to that of the Debye–Waller factor, taking into account the influence of vibrational motion in coherent x-ray scattering. Exchange is assumed to be reduced exponentially with increasing mean squared difference in vibrational or librational elongations at neighbouring arene sites. These squared amplitudes are proportional to T in the high-temperature range. J_1 is a temperature-independent offset, which is necessary to describe $J_{DC}(T)$ of the fluoranthene salt. Its physical origin is not unravelled yet. J_1 is zero for both the perylene and the PY salt.

For the PY salt we suggested the following explanation for the exponential behaviour of $J_{DC}(T)$: at room temperature—i.e. in the regime dominated by CDW fluctuations, which are a precursor for the Peierls transition—the arene molecules perform vibrational and librational motion. In particular, the librational motion leads to a weakening in the overlap of the π orbitals—built up from carbon p electrons—of neighbouring arene molecules. Since these π molecular orbitals are also responsible for the exchange coupling between conduction electrons and defect spins in the stack, J_{DC} is weakened even more, because it is reasonable to assume that the defect sites are amenable to even larger librational amplitudes. On approaching the Peierls transition, this librational motion is frozen in, so the wavefunction overlap between neighbouring molecules is stronger and J_{DC} increases. At T_P the Peierls distortion of the crystal lattice locks in, the π molecular orbital overlap becomes temperature independent, as

does the exchange coupling constant $J_{DC}(T < T_P)$. The larger values of J_{DC} for $(FA)_2PF_6$ and $(PE)_2PF_6 \cdot 2/3THF$ compared to $(PY)_{12}(SbF_6)_7$ go together with a room-temperature ESR line-width for the latter crystals that is larger by a factor of two to three, since there is less exchange narrowing.

This scenario is supported by temperature-dependent NMR measurements of the longitudinal relaxation rates of the ^{19}F nuclei of the counter-ions and the protons of the arene molecules [11, 12]. These measurements showed that the octahedral complex anions in the arene salts exhibit fast re-orientational jumps at room temperature, which freeze-in on cooling down and approaching the Peierls transition. However, similar values of the temperature factors, Q (equation (6)), are derived for all three organic conductors (table 1).

4. Conclusion

We have shown that the familiar bottleneck model, which was established earlier for the spin lattice relaxation of conduction-electron and localized defect spins of various arene radical cation salts in the low-temperature regime, can also be extended to the temperature regime above T_P if one admits a temperature dependence of the intra-stack exchange coupling constant J_{DC}. The exponential increase in J_{DC} on cooling down, which has already been found for the $(PY)_{12}(SbF_6)_7$ salt, can now be confirmed for $(FA)_2PF_6$ as well as for $(PE)_2PF_6 \cdot 2/3THF$. This increase in J_{DC} can also explain the decrease in the absolute value of the ESR line-width reported earlier [3, 4, 8].

The librational motion of the stacked arene molecules (possibly enlarged at the localized defect sites), which freezes in on approaching the Peierls transition, gives a reasonable explanation for the temperature dependence of J_{DC}. Together with the above-mentioned NMR measurements of the longitudinal relaxation rate of the arene protons and the counter-ion ^{19}F nuclei [11, 12], these results indicate the following conclusions. For the locking-in of a Peierls distortion of the crystal lattice, a coupling of the CDWs in neighbouring stacks is a necessary precondition [13]. This inter-stack coupling can be established via the counter-ions, which are located between the stacks. At room temperature it is suppressed by the librational motion of the stacked arene molecules, as well as by the rotational motion of the counter-ions. On cooling down, these motions are reduced in amplitude and frequency, the inter-stack coupling can develop, and the Peierls distortion can lock in.

References

[1] Sachs G, Stöcklein W, Bail B, Dormann E and Schwoerer M 1982 *Chem. Phys. Lett.* **89** 179
[2] Sachs G, Pöhlmann E and Dormann E 1987 *J. Magn. Magn. Mater.* **69** 131
[3] Dormann E and Sachs G 1987 *Ber. Bunsenges. Phys. Chem.* **91** 879
[4] Wolter A, Fasol U, Jäppelt R and Dormann E 1996 *Phys. Rev.* B **54** 12272
[5] Wokrina T, Dormann E and Kaplan N 1996 *Phys. Rev.* B **54** 10492
[6] Müller E, von Schütz J U and Wolf H C 1983 *J. Physique Coll.* **44** C3 1401
[7] Enkelmann V, Morra B S, Kröhnke Ch and Wegner G 1982 *Chem. Phys.* **66** 303
[8] Pongs B and Dormann E 2002 *Phys. Rev.* B **65** 144451

[9] Burggraf M, Dragan H, Gruner-Bauer P, Helberg H W, Kuhs W F, Mattern G, Müller D, Wendl W, Wolter A and Dormann E 1994 *Z. Phys.* B **96** 439

[10] Heeger A J 1969 *Solid State Phys.* **23** 283

[11] Nemec G, Illich V and Dormann E 1998 *Synth. Met.* **95** 149

[12] Kaiser A, Pongs B, Fischer G and Dormann E 2001 *Phys. Lett.* A **282** 125

[13] Desquiotz R, Hofmann M and Dormann E 2000 *Eur. Phys. J.* B **16** 403